A Novel Approach for the Design of a Dry-Tuned Accelerometer/Gyro Instrument

T.J. Ryan*
Teledyne Systems Company, Northridge, California

This paper summarizes the development to date of a dry-tuned accelerator/gyro (DTAG) instrument. In contrast to other types of dry-tuned sensors, the DTAG concept results in a single instrument that provides independent measurements of angular rate about two axes and linear acceleration along two axes. The major features of the feasibility sensor configuation are described and proof of concept test data are presented. An analysis of the DTAG concept is included which determines the sensor design equations, discusses the major mechanization alternatives, and derives the sensitivity of the sensor to error producing mechanisms common to dry-tuned sensors.

Nomenclature

(A,B,C) = principal moments of inertia about x, y, z rotor-fixed axes
A_I,B_I,C_I = principal moments of inertia about x, y, z gimbal-fixed axes
a_x,a_y,a_z = case-referenced linear accelerations
D = damping term associated with motion about the flexure axes
D_{rc} = damping term associated with rotor-to-case motion normal to the spin axis
D_T = damping term associated with rotor-to-case drag torque
j = $\sqrt{-1}$
K_i,K_o = torsional stiffness about inner and outer flexure axes
k_x,k_y,k_z = linear stiffness of rotor-to-shaft suspension along rotor-fixed axes
m_g,m_r = mass of gimbal and rotor, respectively
$n,n_0,n_\cdot$ = spin speed, spin speed for tuned operation, and spin speed for decoupled operation, respectively
Q_0,Q_{2n} = components of quadrature pendulosity
s = Laplace transform variable
T_x,T_y = case-referenced externally applied torques to the rotor
t = time
$(X_g,Y_g,Z_g,X_r,Y_r,Z_r)$ = center of mass location of gimbal and rotor in spinning coordinates
β,γ = space domain and time domain phase angles, respectively, of input mechanical vibrations
Δz = separation between inner and outer flexure axes
$\Delta ln,\Delta 2n$ = amplitude of linear driving motion at spin frequency and twice-spin frequency
ϕ_0 = amplitude of angular driving motion at twice-spin frequency
θ_x,θ_y = case-referenced angular displacement of rotor
$\omega_x,\omega_y,\omega_z$ = case-referenced inertial angular velocity of case
$(\ )$ = complex conjugate operator

Presented as Paper 81-1827 at the AIAA Guidance and Control Conference, Albuquerque, N. M., Aug. 19-21, 1981; submitted Sept. 30, 1981; revision received March 29, 1983.

*Research Scientist, Engineering Department. Member AIAA.

Introduction

THIS paper presents test results and a concept analysis of a dry-tuned accelerometer/gyro (DTAG) in order to demonstrate the feasibility of applying this sensing technology to the mechanization of an inertial grade four-axis multifunction sensor. The development and application of a practical inertial grade multisensor holds the potential for a significant advance in the development of low-cost guidance and control systems. Table 1 compares the number of sensors required for a three-axis inertial measurement unit (IMU) vs single-degree-of-freedom (SDOF) gyros and accelerometers, two-degree-of-freedom (TDOF) gyros and SDOF accelerometers, and four-axis (DTAG) sensors. The reduction in the number of sensors required results in significant savings to the IMU user. Chief among these are:

1) smaller size and weight of the IMU;
2) reduction of the total electronics requirement at the IMU level in comparison with existing technology;
3) increase in reliability by virtue of the reduction in the number of components; and
4) reduced inventory for maintenance due to the reduction in the number of sensors and sensor types.

The DTAG sensor provides measurements of angular rate about two orthogonal axes and acceleration along the same two orthogonal axes as illustrated in Fig. 1. The DTAG concept, a derivative of dry-tuned sensor technology, does not require breakthroughs in materials or material-related technology in order to develop a practical implementation. In a dry-tuned gyro (DTG),[1] the mechanical spring rate of the flexures is offset by the negative spring rate of the gimbal inertias. At the design spin speed, the net spring rate torque is ideally zero for low-frequency rotational inputs. The angular momentum of the rotor provides the desired sensitivity to rate inputs. In the DTAG concept the mechanical spring rate of the flexures is offset by the negative spring rate of both the gimbal and rotor inertias. At the designed spin speed, the net spring rate torque at twice the spin frequency is ideally zero for low-frequency rotational inputs. From a design standpoint, sensitivity to angular rate inputs and linear acceleration inputs are available from five mechanisms: 1) rotor angular momentum; 2) rotor unsymmetrical inertia; 3) rotor axial pendulosity; 4) gimbal axial pendulosity; and 5) rotor asymmetrical inertia.[2]

Rotor angular momentum and rotor axial pendulosity generate sensitivities to angular rate and linear acceleration inputs, respectively. Unsymmetrical rotor inertials[3,4] and gimbal axial pendulosity modulate the case rates and linear acceleration to produce sensitivities at twice the spin frequency. A DTAG sensor can be mechanized in either of two ways. One design concept uses an inertially unsymmetric rotor to provide the desired sensitivity to angular rate at twice-spin frequency and rotor axial pendulosity to generate the desired sensitivity to linear acceleration inputs at low frequency. This concept trades the advantageous characteristics of converting acceleration-dependent gyro uncertainties due to rotor "mass shifts" along the spin axis into an accelerometer scale factor uncertainty for a compensatible rate cross-coupling term in the resulting acceleration signal due to rotor angular momentum. An alternate mechanization utilizes a symmetric rotor to provide the desired sensitivity to angular rate and a combination of both rotor and gimbal pendulosity to generate the desired sensitivity to linear acceleration input at twice-spin frequency.

DTAG Feasibility Sensor Design

In the feasibility demonstration sensor, items 1, 2, and 3 listed above were used to generate the desired sensitivities to angular rate and linear acceleration.

DTAG Comparison with a DTG

A comparison of the DTAG feasibility demonstration sensor response and a DTG response to rate inputs and torque inputs is presented in Fig. 2. In response to applied input rate at a frequency f_ω, the DTAG exhibits a conventional low-frequency response at the same frequency as the input due to the angular momentum. In addition, the DTAG sensor has a twice-spin frequency response at $2n \pm f_\omega$ due to unsymmetric rotor moments of inertia. The upper left-hand side of Fig. 2 illustrates the angular momentum response of a DTG sensor to a rate input at the same frequency. In contrast to a DTG, the rotor in the DTAG feasibility sensor is purposefully made pendulous along the spin axis. The rotor axial pendulosity, when acted upon by a linear acceleration at frequency f_a, applies a torque at the same frequency to the rotor. Both the DTAG sensor and a DTG sensor demonstrate the same response to low-frequency torque, regardless of its origin, as indicated in the lower half of Fig. 2. Since the angular rate inputs are measured separately in the twice-spin frequency domain outputs, it is possible to subtract these angular rate measurements from the measurements in the low-frequency domain, which represent the sum of the applied rate and linear acceleration inputs, in order to obtain two separate outputs proportional to the linear acceleration along the X and Y case axes.

Feasibility Sensor Design

The major subassemblies of the DTAG sensor feasibility design will now be discussed.

Suspension

In a dry-tuned sensor, the suspension assembly is analagous to a Hooke's joint. As illustrated in Fig. 1, the suspension consists of the gimbal and torsion elements or flexures. The inner torsion elements connect the gimbal to the shaft, thereby allowing the gimbal and rotor angular freedom relative to the shaft. The outer torsion axis is orthogonal to the inner torsion axis and allows the rotor angular freedom relative to both the gimbal and the shaft. When the DTAG suspension system and rotor (i.e., the sensitive element) are run at the speed required for tuned operation, the dynamically induced spring rate due to the sensitive element inertias is equal and opposite to the mechanical spring rates of the inner and outer axis torsion elements. The spring rates about the inner and outer flexure axes are determined from Eqs. (10) and (19), which are

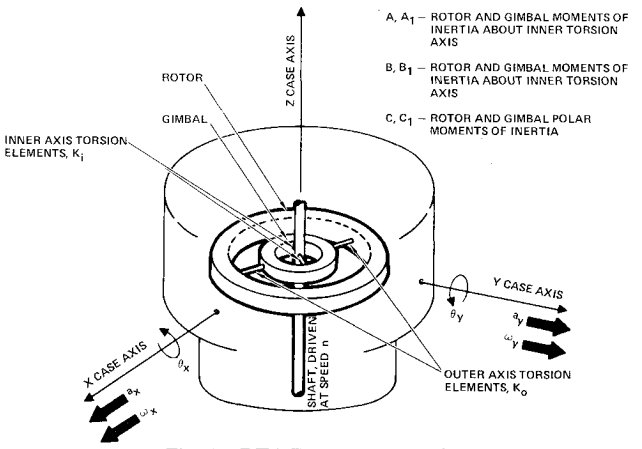

Fig. 1 DTAG sensor conventions.

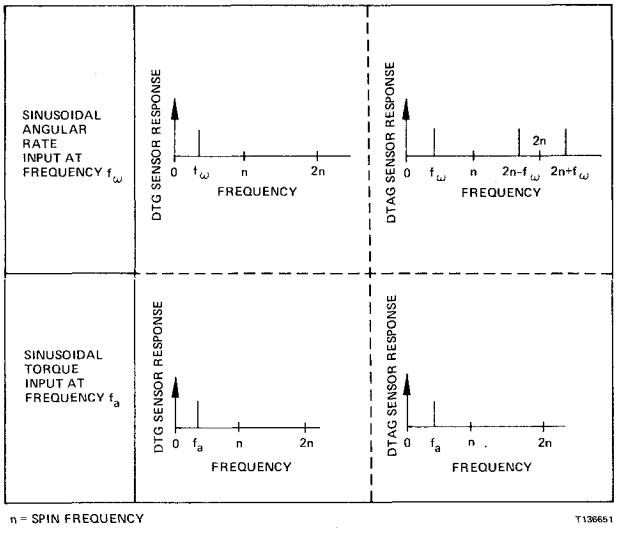

Fig. 2 DTAG feasibility sensor/DTG sensor response comparison.

developed in the DTAG concept analysis. The mechanical design of the suspension considers anisoelastic effects and g-capability in addition to the torsional spring rates about the inner and outer torsion axes.

Rotor

The DTAG rotor design is unique to the concept of simultaneously measuring and separating two axes of angular rate and linear acceleration. Thus, the DTAG feasibility rotor differs from a DTG rotor in two important respects. The rotor is designed to be pendulous along the spin axis. The desired amount of pendulosity is designed into the rotor by controlling the distance along the spin axis between the flexure axes in the suspension and the rotor center of mass. In addition, the rotor is designed to have unequal principal moments of inertia. Figure 3a shows an assembled DTAG rotor. The exploded view of the DTAG rotor in Fig. 3b shows the outer rotor portion to be a sandwich-type structure. The unsymmetrical rotor inertias result from the two annular sectors of high-density material. These annular segments are contained within the cover and ring channel which serve as a windage shield. Inside the outer rotor portion is the torquer return path which contains permanent magnets. The tuning ring provides coarse adjustment of the rotor inertias to achieve the desired tuning condition. Vernier adjustments to the tuning condition, rotor pendulosity, and mass unbalance trim are accommodated by the four rotor weights. The rotor weight inserts provide a self-tooling feature in the assembly of the outer rotor portion.

Pickoffs

The DTAG sensor employs a spin angle pickoff in addition to pickoffs which measure the sensitive element angular deflection. The spin angle pickoff provides twice-spin frequency in-phase and quadrature electronic signals which are required by the caging electronics. The rotating portion of the spin angle pickoff is a disk with 16 slots. The case-fixed portion of the spin angle pickoff is an electro-optic package containing a light-emitting diode and a detector. The spin motion of the shaft causes the slots to chop the light beam. The measure of the spin angle is provided by the detector which senses the intensity of the chopped-light beam.

Pickoffs which measure the rotor and the gimbal angular displacements about the X and Y case-fixed axes are employed in the feasibility sensor. The use of the gimbal pickoffs, an optional design feature, ideally eliminates the necessity for mechanical stability in the pickoff design. A low-frequency rotor displacement with respet to the driven axis forces the gimbal to oscillate at twice-spin frequency. This oscillation occurs about the inner flexure axis. The peak-to-peak amplitude of the resulting twice-spin frequency oscillation equals the rotor low-frequency displacement. Both low-frequency and twice-spin frequency angular displacements of the rotor are sensed by the rotor pickoffs. Variable capacitors mechanize both the rotor and the gimbal pickoffs. The movable portion for the rotor pickoff is the cover for the outer ring sandwich-type structure in Fig. 3b. A separate pickoff ring for the gimbal is included in the suspension design. The case-fixed portion of the capacitive pickoff is mechanized using a two-sided printed circuit board. The pickoff electronic components are mounted on one side of the printed circuit board; the stationary pickoff plates are located on the opposite surface.

Torquer

The function of the torquer mechanism is to exert a controlled moment on the rotor. The magnitude of the controlled moment provides the measure of the inertial angular velocity and linear acceleration sensed by the rotor. The torquer is a permanent magnet voice-coil electromagnetic type. The torquer mechanism consists of two mechanical assemblies: the rotating torquer magnet with return path and the case-fixed torquer coils. Two pairs of coils are used in series per torquer axis. A total of four case-mounted coils provide the capability of exerting controlled moments on the rotor about two orthogonal case-fixed axes.

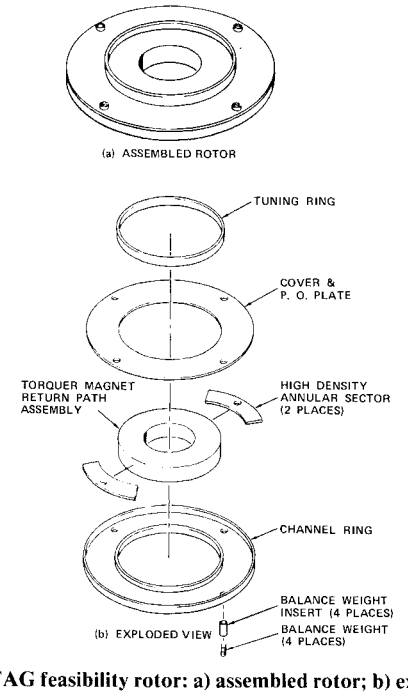

Fig. 3 DTAG feasibility rotor: a) assembled rotor; b) exploded view.

Housing

The DTAG sensor housing serves as a rigid structure to support the sensitive element. It provides precision alignment surfaces for the torquers, the spin bearings, and the mechanical interface with the test fixture of the system. It also provides an electrical interface to the inside of the sensor, a hermetic seal, and magnetic shielding. Commerically available spin bearings, a spin motor, and top and bottom covers comprise the remaining housing elements.

Feasibility Sensor Test Results

Test data on the feasibility sensor configuration were obtained in an electronically caged torque-to-balance operational mode. A comparison of the performance goals with the measured data is presented in Table 2. These goals are not intended to imply any fundamental limitations to the DTAG instrument performance.

Gyro Output Data

The random gyro bias was 0.028 deg/h, which repreesents the average of several runs reduced with an averaging time of 150 s. The randomness in the gyro output vs averaging time has a general $T^{-1/2}$ characteristic for averaging times up to 1000 s. The day-to-day and long-term bias test data constitute the root mean square value of bias repeatability. Day-to-day bias repeatability of 0.17 deg/h for both the X and Y gyro outputs was observed over a one-week period. Long-term bias repeatability of 1.22 and 2.08 deg/h, obtained over an eight-month period, appear to be more strongly affected by electronics than the mechanical sensor, as modifications were being made to the electronics during this period. The total peak-to-peak variation in the measured gyro scale factor was ±65 ppm.

Table 1 Systems considerations: DTAG reduces IMU sensor types and quantities

Sensors	SDOF technologies	TDOF gyros and SDOF accelerometers	Four-axis DTAG
Gyros	3	2	0
Accelerometers	3	3	0
DTAGs	0	0	2
Total sensor count	6	5[a]	2[b]

[a] One redundant rate measurement.
[b] Two redundant measurements—one rate and one acceleration.

Table 2 DTAG sensor test data and comparison with performance goals

Parameter	Performance goal	Test data	Units
Gyro outputs			
Random bias	0.1	0.028	deg/h
Day-to-day bias	0.3	(0.17, 0.17)	deg/h
Long-term bias	1.0	(1.22, 2.08)	deg/h
Scale factor non-linearity	50	±65 (peak-to-peak)	ppm
Accelerometer outputs			
Random bias	100	71	$10^{-6}g$
Day-to-day bias	0.1	(2.01, 0.69)	$10^{-3}g$
Long-term bias	1.0	(2.17, 0.69)	$10^{-3}g$
Scale factor non-linearity	50	±63 (peak-to-peak)	ppm

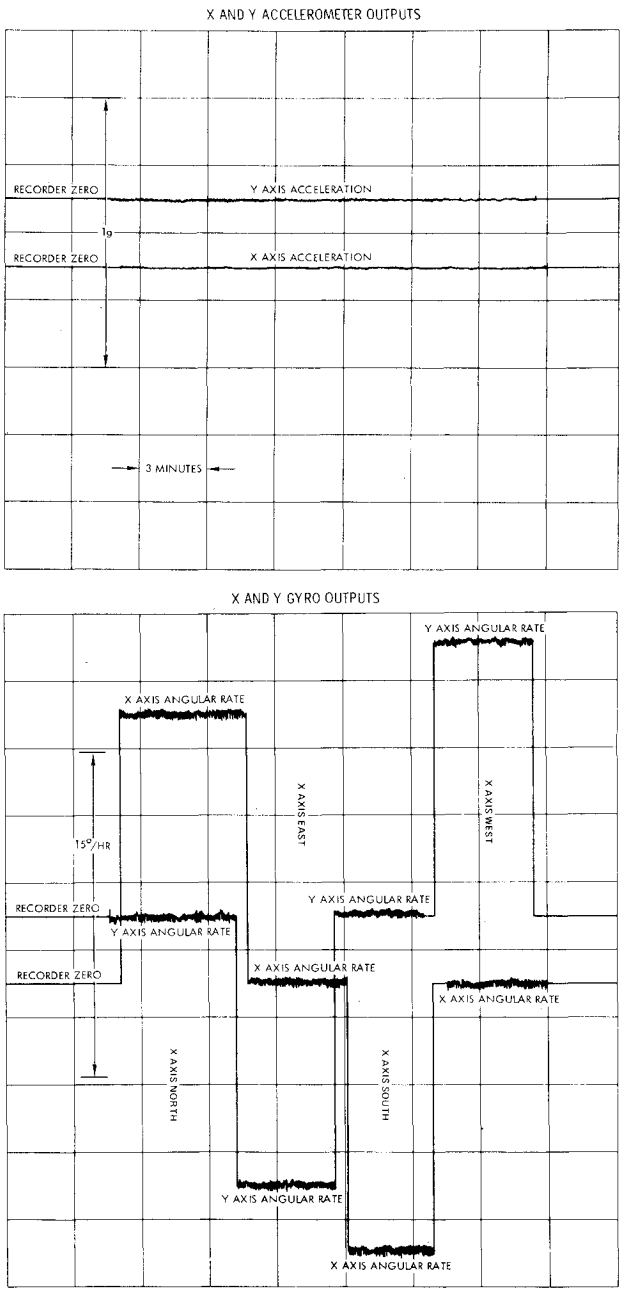

Fig. 4 DTAG instrument outputs for four-point spin axis vertical test demonstates separation of angular rate and linear acceleration.

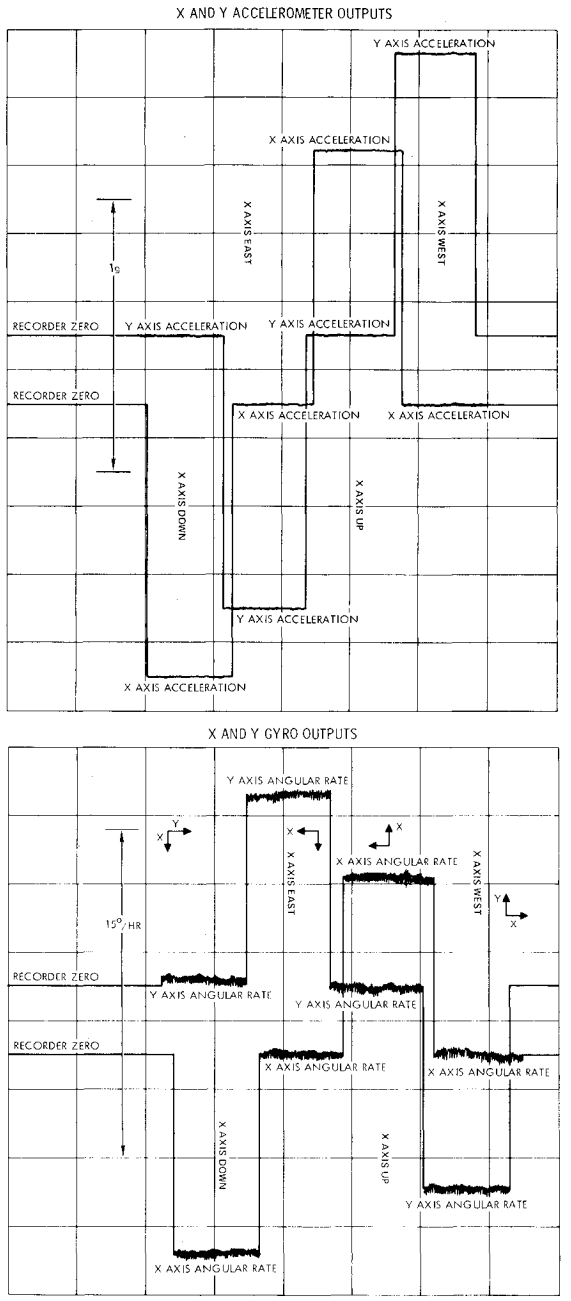

Fig. 5 DTAG instrument output for four-point spin axis horizontal test demonstrates separation of angular rate and linear acceleration.

Accelerometer Output Data

The accelerometer output data were obtained under the same conditions and simultaneously with the gyro output data. The accelerometer random bias of 71 μg's was meausred under the same conditions as the random gyro bias. Day-to-day and long-term accelerometer bias measurements indicate that the accelerometer Y-channel performance exceeds the X-channel. This difference is attributed to limitations in the test electronics. The measured accelerometer scale factor data has a peak-to-peak difference of ± 63 ppm.

Four-Point Output data

Figure 4 illustrates the compensated output for a four-point spin axis vertical test. The upper portion of the figure shows the X and Y accelerometer outputs, while the lower portion of the figure shows the X and Y gyro outputs. No change in the X or Y accelerometer outputs occurred as the sensor axes were positioned along the four cardinal points of north, east, south, and west. The gyro outputs respond to the projection of Earth rate's horizontal component onto the sensing axes.

Figure 5 shows the compensated outputs for a four-point spin axis horizontal test. The upper portion of Fig. 5 shows the response of X and Y accelerometer outputs to Earth's gravity vector as the sensor orientation is changed through the sequence X axis down, east, up, and west. The lower portion of Fig. 5 exhibits the gyro outputs in response to the projection of Earth rate's vertical component onto the X and Y sensing axes.

DTAG Concept Analysis

Background

An understanding of the DTAG is obtained by analyzing the factors which underlie the basic concept of operation as well as the sensitivity to nondesired mechanisms. This analysis is based on a set of dynamic equations that are used to

develop the sensor design constraints and to serve as a basis of evaluating the sensor performance. The dynamic equations of motion in case-fixed coordinates of an elastically supported, multigimbal, tuned gyroscope have been stated by Craig[1] in Eq. (30), with definitions given by Eqs. (35), (38), (39), (42), and (43) in that reference. Craig's results, as modified to describe a single gimbal sensor with inputs to the dynamic system consisting of external torques and case-referenced inertial angular velocity, become:

$$\tau_1(s)\theta_{xy}(s)+\tau_2(s)\bar{\theta}_{xy}(s-j2n)=T_{xy}(s)$$
$$-F_1(s)\omega_{x\dot{y}}(s)-F_2(s)\bar{\omega}_{xy}(s-j2n) \quad (1)$$

where:

$$\tau_1(s)=\tfrac{1}{2}(A+A_1+B)s^2-jn(C+A_1)s+(D+D_{rc})s$$
$$-\tfrac{1}{2}n^2(A_1+B_1-C_1)+\tfrac{1}{2}(K_i+K_0)$$
$$-j(D_T+nD)$$
$$\tau_2(s)=\tfrac{1}{2}(A+A_1-B)s^2-jn(A+A_1-B)s$$
$$-\tfrac{1}{2}n^2(A_1+B_1-C_1)+\tfrac{1}{2}(K_i-K_0)$$
$$F_1(s)=\tfrac{1}{2}(A+A_1-B)s-jn[C+A_1$$
$$-\tfrac{1}{2}(A_1+B_1-C_1)]$$
$$F_2(s)=\tfrac{1}{2}(A+A_1-B)s-\tfrac{1}{2}jn(A_1+B_1-C_1)$$
$$\bar{\tau}_1(s-j2n)=\tfrac{1}{2}(A+A_1+B)s^2-j2n[A+B-C$$
$$+\tfrac{1}{2}(C+A_1)]s+(D+D_{rc})s+\tfrac{1}{2}(K_i+K_0$$
$$-2n^2(A+B-C)-\tfrac{1}{2}n^2(A_1+B_1-C_1)$$
$$+j(D_T-nD-2nD_{rc})$$
$$\bar{\tau}_2(s-j2n)=\tfrac{1}{2}(A+A_1-B)s^2-jns(A+A_1-B)$$
$$+\tfrac{1}{2}(K_i-K_0)-\tfrac{1}{2}n^2(A_1+B_1-C_1) \quad (2)$$

The open-loop transfer function is determined by the simultaneous solution of Eq. (1) and its complex conjugate with the Laplace variable shifted by $s-j2n$ for $\theta_{xy}(s)$.

$$\theta_{xy}(s)=[\bar{\tau}_1(s-j2n)T_{xy}(s)-\tau_2(s)\bar{T}_{xy}(s-j2n)$$
$$+\{\tau_2(s)\bar{F}_2(s-j2n)-\bar{\tau}_1(s-j2n)F_1(s)\}\omega_{xy}(s)$$
$$+\{\tau_2(s)\bar{F}_1(s-j2n)-\bar{\tau}_1(s-j2n)F_2(s)\}\omega_{xy}(s-j2n)]$$
$$\div[\tau_1(s)\bar{\tau}_1(s-j2n)-\tau_2(s)\bar{\tau}_2(s-j2n)] \quad (3)$$

Design Constraints on the Flexture Spring Rates

In the DTAG sensor the sum and the difference of the inner and outer torsion axes spring rates are considered as free parameters that are selected to achieve two design constraints. The first design constraint implements a measure of decoupling between the low-frequency response and the twice-spin frequency response of the sensor to applied torques. The second design constraint determines the spin speed required for tuned operation.

The decoupling condition is achieved by selecting a value for the difference between the inner and outer axes spring rates, such that a low-frequency torque does not give rise to a steady-state pickoff response at twice-spin frequency and, conversely, a twice-spin frequency torques does not cause a steady-state, low-frequency pickoff response. Let the torque applied to the rotor be

$$T_x(t)=T_x(2n)\cos(2nt)-T_y(2n)\sin(2nt)$$
$$T_y(t)=T_x(2n)\sin(2nt)+T_y(2n)\cos(2nt) \quad (4)$$

Then for $T_{xy}(t)=T_x(t)+jT_y(t)$ and substituting Eq. (4), we obtain

$$T_{xy}(t)=T_{xy}(2n)e^{j2nt}$$

taking the Laplace transforms

$$T_{xy}s=\frac{T_{xy}(2n)}{s-j2n} \quad (5)$$

and

$$\bar{T}_{xy}(s-j2n)=\frac{\bar{T}_{xy}(2n)}{s} \quad (6)$$

Substitute Eqs. (5) and (6) into Eq. (3). Then for the condition of no external rate input the pickoff response is given by

$$\theta_{xy}(s)=\frac{\bar{\tau}_1(s-j2n)\dfrac{T_{xy}(2n)}{s-j2n}-\tau_2(s)\dfrac{\bar{T}_{xy}(2n)}{s}}{\tau_1(s)\bar{\tau}_1(s-j2n)-\tau_2(s)\bar{\tau}_2(s-j2n)} \quad (7)$$

The steady-state value of Eq. (7), as calculated from residue theory, is

$$\theta_{xy}(0)=\lim_{s\to 0}\{s\theta_{xy}(s)\}=\frac{-\tau_2(0)\bar{T}_{xy}(2n)}{\tau_1(0)\bar{\tau}_1(-j2n)-\tau_2(0)\bar{\tau}_2(-j2n)} \quad (8)$$

The decoupling condition results when

$$\tau_2(0)=0 \quad (9)$$

Evaluating Eq. (9) results in the first design constraint as summarized by

$$\tfrac{1}{2}(K_i-K_o)=\tfrac{1}{2}n^2(A_1+B_1-C_1) \quad (10)$$

so that the spin speed required to implement the decouplign condition is

$$n_*=\sqrt{\frac{K_i-K_o}{A_1+B_1-C_1}} \quad (11)$$

For the converse situation in which no steady-state, twice-spin frequency response is desired for a low-frequency torque, let

$$T_{xy}(t)=T_{xy}(0) \quad (12)$$

Then the required Laplace transforms of Eq. (12) are given by

$$T_{xy}(s)=\frac{T_{xy}(0)}{s},\qquad \bar{T}_{xy}(s-j2n)=\frac{\bar{T}_{xy}(0)}{s-j2n} \quad (13)$$

Substituting Eq. (13) into Eq. (3) with zero angular velocity results in

$$\theta_{xy}(s)=\frac{\bar{\tau}_1(s-j2n)\dfrac{T_{xy}(0)}{s}-\tau_2(s)\dfrac{-T_{xy}(0)}{s-j2n}}{\tau_1(s)\bar{\tau}_1(s-j2n)-\tau_2(s)\bar{\tau}_2(s-j2n)} \quad (14)$$

The steady-state response of Eq. (14) at the positive twice-spin frequency, as calculated from residue theory, becomes

$$\theta_{xy}(+j2n) = \lim_{s \to +j2n} \{(s-j2n)\theta_{xy}(s)\}$$

$$= \frac{-\tau_2(+j2n)\bar{T}_{xy}(0)}{\tau_1(+j2n)\bar{\tau}_1(0)\bar{\tau}_2(+j2n)\bar{\tau}_2(0)} \quad (15)$$

The decoupling conditions result when

$$\tau_2(+j2n) = 0 \quad (16)$$

Evaluation of Eq. (16) results in the same condition as Eq. (10).

The desired tuning condition imposed in the DTAG concept requires the sensor to have a free integration at the positive twice-spin frequency. Thus, the open-loop transfer function is to have a pole at $s=j2n$. From Eq. (3) it is established that the free integration results when

$$\tau_1(s)\bar{\tau}_1(s-j2n) - \tau_2(s)\bar{\tau}_2(s-j2n)\,|_{s=j2n} = 0 \quad (17)$$

The consistent solution of Eq. (17) with the decoupling constraint specified by Eq. (16) is

$$\tau_1(+j2n) = 0 \quad (18)$$

Evaluation of Eq. (18) with the damping terms neglected results in the second design constraint

$$\tfrac{1}{2}(K_i+K_o) = 2n^2(A+B-C) + \tfrac{1}{2}n^2(A_1+B_1-C_1) \quad (19)$$

Thus, the spin speed required for tuned operation at the positive twice-spin frequency is

$$n_o = \sqrt{\frac{K_i+K_o}{4(A+B-C)+(A_1+B_1-C_1)}} \quad (20)$$

In Eq. (20) it is worth noting in qualitative terms that the DTAG concept requires larger spring rates to achieve the free integration at the tuned twice-spin frequency than the DTG requires to achieve its free integation at low fequency for similar spin speeds. This stems from the presence of both the rotor and the gimbal inertias in the tuning condition. In a DTG the tuning condition is related to the gimbal inertias.[1] As a result of the increased torsional coupling, several of the DTAG sensor torque sensitivities are larger than the corresponding sensitivities of a DTG. A benefit of the twice-spin frequency tuning lies in the fact that the rotor-to-shaft translational stiffness increases with increasing torsional stiffness, which in turn provides the DTAG sensor a high environmental g-capability. The decoupling constraint is unique to the DTAG sensor.

In operation, the spin speed of the DTAG will generally be slightly different from Eqs. (11) and (20). Such differences in the spin speed have a small effect on the tuned twice-span frequency resonant condition. This effect can be analyzed by considering Eq. (17) in more detail. Let

$$\tfrac{1}{2}(K_i+K_o) = 2n_o^2(A+B-C) + \tfrac{1}{2}n_o^2(A_1+B_1-C_1)$$

$$\tfrac{1}{2}(K_i-K_o) = \tfrac{1}{2}n_*^2(A_1+B_1-C_1)$$

$$s = +j2n + \delta\omega_r$$

$$s^2 = -4n^2 - 4n\delta\omega_r$$

$$n_0^2 - n^2 \simeq 2n\delta n_o$$

$$n_*^2 - n^2 \simeq 2n\delta n_* \quad (21)$$

Then direct substitution of Eqs. (21) and (2) into Eq. (17), neglecting damping terms and simplifying, results

$$\frac{\delta\omega_r}{2n} \simeq 2\left(\frac{A+B-C}{C+A_1}\right)\left|\frac{1+\frac{1}{4}\frac{A_1+B_1-C_1}{A+B-C}}{1+2\frac{A+B-C}{C+A_1}}\right|\left[\left(\frac{\delta n_0}{n}\right)\right.$$

$$+2\left(1+\tfrac{1}{4}\frac{A_1+B_1-C_1}{A+B-C}\right)\left(\frac{\delta n_0}{n}\right)^2$$

$$\left.-\tfrac{1}{2}\left(\frac{A_1+B_1-C_1}{A+B-C}\right)\left(\frac{K_i-K_o}{K_i+K_o}\right)\left(\frac{\delta n_*}{n}\right)^2\right] \quad (22)$$

By design, the ratio $A+B-C/C+A_1$ is made significantly less than unity and the remaining ratios are of order unity or less. Then for practical tolerances placed on the mechanical parameters, which implement the tuning and decoupling conditions, the resulting errors in the tuned twice-spin frequency are no larger than second order.

Torque Sensitivity Analysis

In closed-loop torque to balance operation the DTAG electronic servo provides torques that maintain the electronic pickoff signals at their electronic nulls. This is accomplished by providing active feedback in bandwidths centered at low frequency and at the positive twice-spin frequency. The torque which the electronic servos provide are determined in the following paragraphs for the sequentially analyzed conditions of a constant case angular velocity, a fixed amplitude twice-spin frequency angular vibration, steady-state rotor offsets, a constant case acceleration, fixed-amplitude linear mechanical vibrations, and anisoelastic effects.

Sensitivity to Constant Input Angular Velocity

Let the input angular velocity have projections $\omega_x(0)$ and $\omega_y(0)$ along the positive case X and Y axes, respectively. Then

$$\omega_{xy}(t) = \omega_{xy}(0) \quad (23)$$

taking the Laplace transforms

$$\omega_{xy}(s) = \frac{\omega_{xy}(0)}{s}, \qquad \bar{\omega}_{xy}(s-j2n) = \frac{\bar{\omega}_{xy}(0)}{s-j2n} \quad (24)$$

The servotorque required to maintain the pickoff signals at null is calculated by applying Eq. (1) to this condition. Substituting Eq. (24) into Eq. (1) with the pickoff angles set to zero results in

$$T_{xy}(s) = F_1(s)\frac{\omega_{xy}(0)}{s} + F_2(s)\frac{\bar{\omega}_{xy}(0)}{s-j2n} \quad (25)$$

The steady-state torque of Eq. (25) in the low-frequency band and in the positive twice-spin frequency band, as calculated from residue theory, is given by

$$T_{xy}(0) = \lim_{s-0}\{sTxy(s)\} = F_1(0)\omega_{xy}(0) \quad (26)$$

$$T_{xy}(+j2n) = \lim_{s \to +j2n}\{(s-j2n)T_{xy}(s)\} = F_2(+j2n)\bar{\omega}_{xy}(0) \quad (27)$$

Evaluating the basic definitions given by Eq. (2) under the conditions specified by Eqs. (26) and (27), we find

$$T_{xy}(0) = -jn[C+A_1-\tfrac{1}{2}(A_1+B_1-C_1)]\omega_{xy}(0)$$

$$T_{xy}(+j2n) = jn[A+A_1-B-\tfrac{1}{2}(A_1+B_1-C_1)]\bar{\omega}_{xy}(0) \quad (28)$$

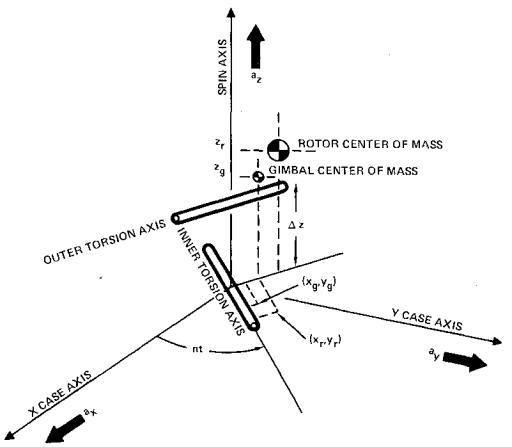

Fig. 6 Conventions for mass sensitive calculations.

where $T_{xy}(0)$ is the torque required to process the sensor's net angular momentum at the specified rate and $T_{xy}(+j2n)$ is the magnitude of the ac torque required to balance the effect of the unsymmetrical rotor inertias. In a symmetric rotor design, the $T_{xy}(+j2n)$ rate sensitivity torque is set to a nominal design value of zero.

Sensitivity to Constant Amplitude Twice-Spin Frequency Angular Vibrations

One characteristic common to rotating tuned sensors is a sensitivity to synchronous input angular motion normal to the spin axis which occurs at twice the shaft spin frequency. Let the amplitude of the external drive motion be ϕ_0 with components along the X and Y case axes given by

$$\phi_x(t) = \phi_0 \sin(2nt+\gamma)\cos\beta$$

$$\phi_y(t) = \phi_0 \sin(2nt+\gamma)\sin\beta$$

$$\phi_{xy}(t) = \phi_0 e^{j\beta}\sin(2nt+\gamma)$$

$$\phi_{xy}(s) = \frac{\phi_0 e^{j\beta}}{j2}\left(\frac{e^{j\gamma}}{s-j2n} - \frac{e^{-j\gamma}}{s+j2n}\right) \tag{29}$$

For ϕ_0, a small amplitude angular input, the case rates are given by

$$\omega_x(t) \simeq \frac{d\phi_x(t)}{dt} \qquad \omega_y(t) \simeq \frac{d\phi_y(t)}{dt} \tag{30}$$

The Laplace transforms of the input rates become

$$\omega_{xy}(s) = \phi_0 n e^{j\beta}\left(\frac{e^{j\gamma}}{s-j2n} + \frac{e^{-j\gamma}}{s+j2n}\right)$$

$$\bar{\omega}_{xy}(s-j2n) = \phi_0 n e^{-j\beta}\left(\frac{e^{j\gamma}}{s-j4n} + \frac{e^{-j\gamma}}{s}\right) \tag{31}$$

Under a torque-to-balance servo restraint, a general expression for the pickoff response is

$$\theta_{xy}(t) = \theta_{xy}(-j2n)e^{-j2nt} + \theta_{xy}(+j4n)e^{j4nt} \tag{32}$$

taking the Laplace transforms

$$\theta_{xy}(s) = \frac{\theta_{xy}(-j2n)}{s+j2n} + \frac{\theta_{xy}(+j4n)}{s-j4n}$$

$$\bar{\theta}_{xy}(s-j2n) = \frac{\bar{\theta}_{xy}(-j2n)}{s-j4n} + \frac{\bar{\theta}_{xy}(+j4n)}{s+j2n} \tag{33}$$

Substituting Eqs. (31) and (33) into Eq. (1), and evaluating the resulting expression for the steady-state torque components at $s=0$, $+j2n$, $-j2n$, and $+j4n$ by analogy with Eqs. (26) and (27), leads to a set of four simultaneous algebraic equations.

$$T_{xy}(0) = F_2(0)\phi_0 n e^{-j(\beta+\gamma)}$$

$$T_{xy}(+j2n) = F_1(+j2n)\phi_0 n e^{j(\beta+\gamma)}$$

$$T_{xy}(-j2n) = \tau_1(-j2n)\theta_{xy}(-j2n) + \tau_2(-j2n)\bar{\theta}_{xy}(+j4n) + F_1(-j2n)\phi_0 n e^{j(\beta-\gamma)}$$

$$T_{xy}(=j4n) = \tau_1(+j4n)\theta_{xy}(+j4n) + \tau_2(+j4n)\bar{\theta}_{xy}(-j2n) + F_2(+j4n)\phi_0 n e^{-j(\beta-\gamma)} \tag{34}$$

The solution to Eq. (34) is facilitated by the following assumptions. The servo is not capable of supplying rebalance torque at $s=-j2n$ and $s=+j4n$. The DTAG is operated at the tuned Eq. (20) and decoupled Eq. (11) conditions with the damping terms set to zero. The ratios of $A+B-C/C+A_1$ and $A_1+B_1-C_1/C+A_1$ are very much less than unity. The functions F_1, F_2, τ_1 and τ_2 are evaluated from Eq. (2) so that we obtain

$$T_{xy}(0) = -\tfrac{1}{2}jn^2(A_1+B_1-C_1)\phi_0 e^{-j(\beta+\gamma)}$$

$$T_{xy}(+2jn) = jn^2[(A+B-C)+\tfrac{1}{2}(A_1+B_1-C_1)] \times \phi_0 e^{j(\beta+\gamma)}$$

$$\theta_{xy}(-j2n) \simeq -\tfrac{1}{2}j\phi_0 e^{j(\beta-\gamma)}$$

$$\theta_{xy}(+j4n) \simeq 0 \tag{35}$$

Notice in Eq. (35) that the amplitude of the pickoff response is equal to the negative input driving motion at $s=-j2n$ in Eq. (29). The pickoff response at $s=+j2n$ is zero due to the free integration at this frequency which results from the tuning condition. In comparison, a DTG evaluated under the same condition of driven input motion, one finds that the ampitude of the low-frequency torque is very nearly equal to one half the value appearing in Eq. (35). In addition the free integration in a DTG which occurs at low-frequency results in a pickoff response equal to the negative of the total driving motion at twice-spin frequency.

Sensitivity to Rotor Offset Angles

The rotor offset angle is the included angle between the driven axis established by the shaft and its mechanical supports and the spin axis of the elastically supported and gimballed rotor. For a sensor configuation in which the case-fixed pickoffs sense the rotor angular position with respect to the sensor case, the pickoff outputs are proportional to the angle $\theta_{xy}(t)$. In torque-to-balance servo operation, rotor offset angle may result from changes in either the mechanical or the electrical null of the pickoff transducer and its associated electronics. Such null offsets contain both low-frequency and twice-spin frequency components. The resulting tortque sensitivity is determined from Eq. (1) with the input rate set to zero.

For the case of low-frequency offsets, let

$$\theta_{xy}(t) = \theta_{xy}(0) \tag{36}$$

taking the Laplace transforms

$$\theta_{xy}(s) = \frac{\theta_{xy}(s)}{s} \qquad \bar{\theta}_{xy}(s-j2n) = \frac{\bar{\theta}_{xy}(0)}{s-j2n} \tag{37}$$

The expression for torque sensitivity results by substituting Eq. (37) into Eq. (1). Then in analogy with Eqs. (26) and (27), and making use of the definitions, Eq. (2), the decoupling condition, Eq. (10), and the approximations in Eq. (21), we find

$$T_{xy}(0) = [K_0 + (A_1 + B_1 - C_1)n\delta n_0 - j(D_T + nD)]\theta_{xy}(0)$$

$$T_{xy}(+j2n) = [(A_1 + B_1 - C_1)n\delta n_*]\bar{\theta}_{xy}(0) \quad (38)$$

For offsets at the tuned twice-spin frequency, let

$$\theta_{xy}(t) = \theta_{xy}(+j2n)e^{j2nt} \quad (39)$$

So that the Laplace transforms become

$$\theta_{xy}(s) = \frac{\theta_{xy}(+j2n)}{s - j2n}$$

$$\bar{\theta}_{xy}(s - j2n) = \frac{\bar{\theta}_{xy}(+j2n)}{s} \quad (40)$$

Then by following the same procedures outlined for the low-frequency offsets, we determine the torque sensitivities to twice-spin frequency rotor offsets to be

$$T_{xy}(0) = [(A_1 + B_1 - C_1)n\delta n_*]\bar{\theta}_{xy}(+j2n)$$

$$T_{xy}(+j2n) = \{[4(A + B - C) + (A_1 + B_1 - C_1)]n\delta n_0 + j[n(D + 2D_{rc}) - D_T]\}\theta_{xy}(+j2n) \quad (41)$$

The low-frequency torque sensitivity to low-frequency rotor offsets, as expressed by Eqs. (38), contains three terms. The dominant term is the fixed spring rate about the outer flexure axis. This term results from the absence of a free integration in the DTAG sensor at low frequency. A smaller spring rate term is present, which is proportional to the difference between the spin speed required by the decoupling design constraint and the operating spin speed. In addition to the spring rate terms, damping terms resulting from drag torques on the rotor and damping associated with the motion about the inner and outer flexure axes are present. For a fixed mechanical configuration the torque sensitivity is directly proportional to the low-frequency rotor offsets. The low-frequency stability of the rotor offset is dependent upon the mechanical stability of the driven axis and the mechanical stability of the pickoff transducer in addition to the electronic stability of the transducer. The implied requirement for mechanical stability in the driven axis and in the pickoff transducer in Eqs. (38) can be eliminated through the use of a gimbal pickoff.

The positive twice-span frequency torque sensitivities summarized by Eqs. (38) and (41) represent the residual coupling between low-frequency rotor offsets and twice-spin frequency torques and between twice-spin frequency rotor offsets and low-frequency torques when the decoupling design constraint, Eq. (9), is not preceisely met. These sensitivities can be trimmed by a sensor calibration procedure when the gimbal design includes provision to adjust the gimbal inertias.

The twice-spin frequency torque sensitivity in Eq. (41) to twice-spin frequency rotor offests contains a spring rate term and a damping term. The spring rate term is proportional to the difference between the spin speed required for tuned operation and the operating spin speed. This term can be made acceptably small by providing the capability to adjust the rotor inertias, which reduces the difference between the spin speed for tuned operation and the operating speed. The damping term contains contributions from the drag torque, motion about the flexure axes, and the rotor-to-case damping. In principal, twice-spin frequency rotor offsets are insensitive to the mechanical stability of the pickoff as well as to the mechanical stability of the driven shaft axis.

Sensitivity-to-Linear Accelerations

The DTAG sensitivity-to-linear acceleration results from two mechanisms. The first is mass unbalance in the gimbal and in the rotor with respect to the flexure axes. Torques due to mass unbalance can be controlled in a sensor design by providing means to adjust the gimbal and rotor mass balance during sensor calibration. The second meachanism is generally referred to as quadrature pendulosity. Quadrature pendulosity is attributed to imperfections and misalignments in the elements which comprise each flexure axis. Torques resulting from quadrature pendulosity have a line of aciton which is colinear with the component of acceleration or gravity along the flexure axis.

A general expression for the torque acting on the rotor due to these two mechanisms has been derived by Craig[5] as Eq. (68) for sensor configurations employing multiple gimbals. This result is presented as Eq. (42) for a single gimbal configuration.

$$T_{xy}(t) = (Q_0 - jP_0)a_{xy}(t) + (Q_{2n} + jP_{2n})\bar{a}_{xy}(t)e^{j2nt} + (P_a + jP_b)a_z(t)e^{jnt} \quad (42)$$

The components of quadrature pendulosity along the inner and outer flexure axes are, respectively, $Q_0 + Q_{2n}$ and $Q_0 - Q_{2n}$. For the conventions in Fig. 6 the mass unbalance terms are related to the parameters in Eq. (42) by

$$P_0 = m_r z_r - \tfrac{1}{2}m_r z + \tfrac{1}{2}m_g z_g$$

$$P_{2n} = \tfrac{1}{2}(m_r \Delta z + m_g z_g)$$

$$P_a = -m_r y_r - m_g m_g$$

$$P_b = m_r x_r \quad (43)$$

For $a_{xy}(t) = a_{xy}(0)$ and $a_z(t) = 0$, the steady-state torque components at low frequency and at the tuned twice-spin frequency become

$$T_{xy}(0) = (Q_0 - jP_0)a_{xy}(0)$$

$$T_{xy}(+j2n) = (Q_{2n} + jP_{2n})\bar{a}_{xy}(0) \quad (44)$$

In a DTG the portion of the torque sensitivities expressed by Eq. (44) due to mass unbalance along the spin axis are most commonly set to nominal values of zero with design provision to trim the residual mass unbalance during sensor calibration. In the DTAG sensor concept the designer seeks to emphasize the spin axis mass unbalance sensitivity by selecting a nonzero nominal value for either P_0 or P_{2n}. When the P_0 term is emphasized, the primary contributor is rotor axial predulosity. If the designer emphasizes the P_{2n} term the primary contributor is gimbal axial pendulosity. In either a DTG or a DTAG the residual effects of quadrature pendulosity give rise to a compensatable instrument coefficient.

Sensitivity to Mechanical Vibrations Along the Spin Axis at Spin Frequency

Disturbance torques from this mechanism exist only in the presence of mechanical vibrations which are collinear with the spin axis and synchronous with the operating spin speed and act upon the radial mass unbalance in the sensitive element. For

$$a_{xy}(t) = 0 \quad \text{and} \quad a_z(t) = -\tfrac{1}{2}\Delta_{ln}n^2\sin(nt + \gamma)$$

where Δ_{ln} is the peak-to-peak amplitude of the mechancial vibration, the resulting torque sensitivity is determined by

substituting into Eq. (42). The resulting expressions for the steady-state torque components at low frequency and at the tuned twice-spin frequency are given by

$$T_{xy(0)} = \tfrac{1}{4}\Delta_{1n} n^2 (P_b - jP_a) e^{-j\gamma}$$

$$T_{xy}(+j2n) = \tfrac{1}{4} j\Delta_{1n} n^2 (P_a + jP_b) e^{j\gamma} \quad (45)$$

The magnitude of these sensitivities is controlled by providing adjustments so that both P_a and P_b can be decreased to within a predetermined tolerance. Residual radial mass unbalance acted upon by synchronous mechanical vibrations at the operating spin speed contributes to the bias stability in either a DTG or a DTAG.

Sensitivity to Mechancial Virbrations Normal to the Spin Axis at Twice-Spin Frequency

For a twice-span frequency mechanical vibration of peak-to-peak amplitude, Δ_{2n}, whose orientation in the plane of the X and Y case axes is at an angle β with respect to the positive case axis, the corresponding accelerations are $a_{xy}(t) = -\Delta_{2n} 2n^2 \sin(2nt+\gamma) e^{j\beta}$ and $a_z(t) = 0$. Then by substituting into Eq. (42) the steady-state torque components at low frequency and at the tuned twice-spin frequency are as given by

$$T_{xy}(0) = \Delta_{2n} n^2 (P_{2n} - jQ_{2n}) e^{-j(\beta+\gamma)}$$

$$T_{xy}(+j2n) = \Delta_{2n} n^2 (P_0 + jQ_0) e^{j(\beta+\gamma)} \quad (46)$$

The torque sensitivity in Eqs. (46) due to the quadrature pendulosity can only be eliminated in designs employing a minimum of three gimbals.[5] Thus the quadrature components in a single gimbal DTG or DTAG are acted upon by variations in the indigenous levels of twice-spin frequency mechanical vibrations, which result in a contribution to the instrument's bias stability. In the DTAG sensor either the P_0 or P_{2n} direct mass unbalance terms are emphasized as noted previously. This results in a contribution to the bias instability at either the tuned twice-spin frequency DTAG instrument output or the low-frequency DTAG instrument output depending upon whether the rotor axial pendulosity or the gimbal axial pendulosity is selected as the mechanism for providing the desired sensitivity-to-case accelerations.

Sensitivity to Anisoelastic Effects

In a dry-tuned sensor the anisoelastic mechanism is related to differences between the rotor-to-shaft translational stiffness along the spin axis, the inner flexure axis, and the outer flexure axis. For configurations in which the mass of the gimbal is neglegible in comparison with the mass of the rotor, the torque sensitivity at low frequency and at the tuned twice-spin frequency are given by

$$T_{xy}(0) = -j\left[\frac{1}{k_z} - \tfrac{1}{2}\left(\frac{1}{k_x - n^2 m_r} + \frac{1}{k_y - n^2 m_r}\right)\right] \times m_r^2 a_{xy}(0) a_z(0)$$

$$T_{xy}(+j2n) = \tfrac{1}{2} j\left[\frac{1}{k_x - n^2 m_r} - \frac{1}{k_y - n^2 m_r}\right] \times m_r^2 a_{xy}(0) a_z(0) \quad (47)$$

The parameters k_x, k_y, k_z are linear spring constants that describe the stiffness of the rotor center of mass with respect to the shaft along the inner flexure axis, the outer flexure axis, and the spin axis, respectively.

Conclusion

This paper presents results which demonstrate the technical feasibility of applying dry-tuned sensor technology to the development of a four-axis multifunction sensor capable of providing two outputs proportional to linear acceleration and two outputs proportional to angular rate. The performance levels of the gyro and accelerometer outputs are consistent with requirements for a broad range of inertial applications.

Acknowledgment

This work was supported in part by AFAL, AFFDL, and AFATL under Contracts F33615-76-C-1076 and F3615-77-C-1147 and by MIRADCOM under Contract DAAK40-77-C-0091.

The concept for this sensor design was originated by H.F. Erdley. J. Dizon, K. Green, R. Hunter, R. Irvine, G. Lewis, F. McNair, J. Ritter, and J. Sammartano made significant contributions to the program.

References

[1] Craig, R.J.G., "Theory of Operation of an Elastically Supported, Tuned Gyroscope." *IEEE Transactions of Aerospace and Electronic Systems,* Vol. AES-8, No. 3, May 1972, pp. 280-288.

[2] Erdley, H.F., Lipman, J.S., and Shapiro, S., "Vibra-Rotor Gyroscopes," U.S. Patent No. 3,463,016, Aug. 26, 1969.

[3] Magnus, K., *Gyrodynamics,* Springer-Verlag, New York, 1974, p. 10.

[4] Arnold, R.N., and Maunder, L., *Gyrodynamics and its Engineering Applications,* Academic Press, New York, 1961, pp. 297-305, 423-425.

[5] Craig, R.J.G., "Theory of Errors of a Multigimball, Elastically Supproted, Tuned Gyroscope," *IEEE Transactions on Aerospace and Electronic Systems,* Vol. AES-8, No. 3, May 1972, pp. 289-297.